Research Article

The Panama Low-Level Jet: extension, annual cycle and modes of variation

Silvio Andrés Ordóñez-Zúñiga[1] , **Marco Correa-Ramírez[1]**
Constanza Ricaurte-Villota[1] **& Martha Bastidas-Salamanca[1]**
[1]Instituto de Investigaciones Marinas y Costeras, José Benito Vives de Andreis (INVEMAR)
Santa Marta, Distrito Turístico, Histórico y Cultural, Colombia
Corresponding author: Silvio Andrés Ordónez-Zúñiga (silvio.ordonez@invemar.org.co)

ABSTRACT. The Panama Low-Level Jet (PLLJ) is the inter-isthmic jet closest to the equator, whose activation modifies circulation, sea surface temperature, and climate in most Eastern Tropical Pacific off Colombia. Through analysis of 26 years (1992-2018) of sea wind data, the jet extent and its main frequencies of variability were determined, in addition to its relationship with phenomena of climatic variability. The area of direct influence of the jet was estimated to be 59,295.34 km², being located between 4°37'48" and 9°0'0"N. The PLLJ has activated annually from December to April with intense intra-seasonal variability (with frequencies between one to five months) and inter-annual perturbations associated with El Niño Southern Oscillation (ENSO) events. During warm ENSO events, the PLLJ activity lasts around two months more (from mid-November to the end of May), and its spatial extent increases southerly, reaching around 2°N. Additionally, during warm ENSO years, there is an extemporaneous activation of PLLJ in the boreal summer, possibly linked to the intensification of the North Trade Winds over the Caribbean basin in the middle of the year. The entry of Caribbean winds in unusual seasons changes the seasonal pattern of the PLLJ and increases its influence in the Eastern Tropical Pacific during the warm ENSO phases.

Keywords: Panama Low-Level Jet; winds; frequency analysis; wavelet; satellite; reanalysis; Eastern Tropical Pacific

INTRODUCTION

A low-level jet (LLJ) is a stream of air below 600 hPa whose periods of intensification and relaxation are modulated by pressure gradients and temperature differences that occur in geographically separated parcels or between the continent and the ocean. The LLJs can strongly influence meteorological systems on a synoptic scale, contributing significantly to the local climate in the tropics and high latitudes (Amador 1998). When LLJs occur over the sea, they can affect the hydrography of the water column, decrease the sea surface temperature (SST) and increase marine biological productivity (Chelton et al. 2000a), or even produce upwelling (O'Dea et al. 2012, Smith et al. 2014). Moreover, they are responsible for transporting heat and water vapor poleward (Stensrud 1996). Among the most well-known tropical LLJs is the Somali Jet. A south-westerly jet with maximum speed near 850 hPa that feeds moisture to the South Indian monsoon; this jet results from the cross-equatorial flow that is bounded by the East African mountains to the west and occurs during the summer (most intense from June to August) over northern Madagascar and off the coast of Somalia (Laing & Evans 2010).

Another example is the African Easterly Low-Level Jet (AEJ) with a maximum of 700 and 600 hPa and between 13 and 17°N with wind speeds of 10-25 m s⁻¹. The AEJ is well defined from April to November but is strongest during the West African monsoon, between June and September. The existence of this jet is associated with the strong reversal in the typical meridional temperature gradient over the African continent during the summer (usually warmer at the equator) (Laing & Evans 2010); this jet is also responsible for the transport of Saharan dust to South America (Francis et al. 2020). The LLJ phenomena also occur in East Asia, where deep convection and heavy precipitation are persistent where a jet at 850 hPa interacts with the Mei-yu/Baiu Front, which is a persis-

tent, nearly stationary, and weak baroclinic zone in the lower troposphere located over the east coast of China and Taiwan (Stensrud 1996). They are also present during the Indian summer monsoon, where an LLJ is primarily responsible for transporting moist air and modulates rainfall and local climate (Rai & Dimitry 2017). The trade wind regime is also known as the Caribbean Low-Level Jet (CLLJ), an easterly jet with a maximum speed of 925 hPa prevalent over the Caribbean Sea between 12-14°N and 70-75°W mainly during February and July (Muñoz et al. 2008). In high latitudes, studies have shown that the development of LLJs can be forced by the baroclinicity induced in coastlines and the sea-ice edges, by katabatic flows over continental ice sheets, and topography restrictions to wind flow. In these locations, LLJs are more common over land than over open sea areas, and that most of these phenomena are associated with either sea ice or topography (Renfrew & Anderson 2006, Tuononen et al. 2015). Such LLJs may affect the motion of the sea ice margin, which further affects the sea ice mass balance, especially during boreal spring and summer (Langland et al. 1989, Jakobson et al. 2013).

Between the Eastern Tropical Pacific and the Atlantic, the pressure gradients at 925 hPa during the boreal winter accelerate the winds towards the south through the gaps present in the Central American mountains generating three strong inter-isthmic wind jets: Tehuantepec (Mexico), Papagayo (Nicaragua) and Panama (Romero-Centeno et al. 2003, Xie et al. 2005). Despite sharing a similar origin, the variability of these three jets is not completely correlated with each other (Chelton et al. 2000a,b). The Tehuantepec Jet has a greater influence on synoptic wind patterns that migrate from west to east across the Gulf of Mexico and northwest Caribbean Sea (Chelton et al. 2000b). However, the expansion and intensification of the Azore's high pressure have been observed accelerating the Tehuantepec and Papagayo jets in the middle of the boreal summer (Romero-Centeno et al. 2003, Small et al. 2007). The Papagayo and Panama jets are more affected by variations in the trade winds that extend from the Caribbean and are decoupled from the low-level atmospheric variability in the mid-latitudes (Chelton et al. 2000a).

The Panama Low-Level Jet (PLLJ) is the inter-isthmic jet located further south and closest to Ecuador, formed during boreal winter over the Panama Bay region in the Eastern Tropical Pacific off Colombia (ETPC) at 925 hPa (Devis-Morales et al. 2008). The PLLJ begins in late November, reaches its highest intensity with an approximate maximum speed between 7 and 10 m s^{-1} over the Panama Bay in January, then gradually decreases from February until disappearing in June (Rueda-Bayona et al. 2007). The PLLJ intensification occurs after the other two inter-isthmic jets (Chelton et al. 2000a, Mora 2017) when the intertropical convergence zone (ITCZ) reaches its southernmost position between February and March (Forsbergh 1969, Rodríguez-Rubio et al. 2003). Its activation changes the cyclonic ocean circulation in the ETPC established in the boreal winter (December to February), making it anticyclonic in the boreal summer (June to August) (Rodríguez-Rubio et al. 2003, Devis-Morales et al. 2008).

Although the PLLJ has been characterized in previous studies (Chelton et al. 2000a, Rueda Bayona et al. 2007, Devis-Morales et al. 2008, Mora 2017), few research studies have described in detail its extent and scales of temporal variability. It has been observed that all Central American wind jets show differences between the warm and cold events associated with the El Niño Southern Oscillation (ENSO) (Alexander et al. 2012), but in the case of the PLLJ, the ENSO variability is even inverse to that observed in the other inter-isthmic jets (Yang et al. 2017). Considering that the ENSO phenomenon is the strongest mode of climatic variability in the tropics (Pezzi & Cavalcanti 2001, Turner et al. 2005) and regionally recognized for modulating variations in precipitation (Ropelewski & Halpert 2002, Sáenz & Durán-Quesada 2015). This study analyses the regional influence of the PLLJ to understand the mechanisms by which alterations from ENSO to PLLJ can affect ocean circulation, sea surface temperature, and weather in ETPC.

MATERIALS AND METHODS

To analyze the variability of the PLLJ in the study area (82-77°W, 0-9°N, Fig. 1) the database from Institut Français de Recherche pour l'Exploitation de la Mer (IFREMER) and Center ERS d'Archivage et de Traitement (CERSAT) was used. These data included wind components (meridional and zonal) downloaded from the Copernicus portal with a sampling period between 1992 to 2018. The satellite wind data every 6 h (00:00, 06:00, 12:00 and 18:00 h UTC) and a horizontal grid spacing of 0.25° (~27 km) merge all remotely sensed surface wind products derived from currently available scatterometers and radiometers, through an objective interpolation method. The downloaded wind database is a level 4 (L4) product since it is derived from the re-processing of satellite L2 observations and combined with the ERA-interim wind analysis from January 1992 onwards. The study area is a section of the Pacific dominated by two wind systems, the PLLJ in boreal winter and the South West Trade Winds (SWTW), which last the rest of the year.
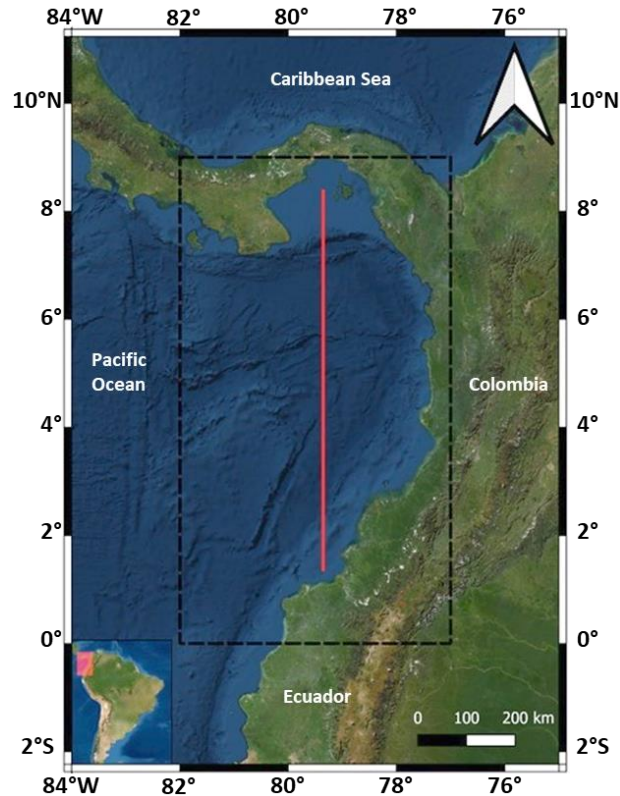
Figure 1. The study area map is surrounded by the black dotted line (82-77°W, 0-9°N) and is represented as the red fraction in the South America figure at the bottom left. The solid red line is the latitudinal transect (79°22'30"W, 8°22'30"-1°22'30"N), on which the convolutional spectrum of Figure 5 was calculated.

The extension of the PLLJ using the wind fields is determined by two approaches, one based on variability and the other on coherence. In the variability-based approach, the extent of the PLLJ was determined as the area of high variability (standard deviation) of the winds within the Panama Bay, delimited by the 2.10 std isoline threshold, which corresponds to the value where the greatest spatial gradient is observed in the field of the standard deviation of the winds. In the coherence approximation, the PLLJ area is determined as the region where the winds show similar behavior and the strongest positive association concerning the winds at the point of observed maximum wind variability (or standard deviation) in the PLLJ region (from now on $PLLJ_{max}$), located at 79°22'30"W and 7°22'30"N. Therefore, the coherence area is defined where the wind correlation with the $PLLJ_{max}$ is positive and significant above 99% ($P < 0.01$).

The jet annual cycle and its initiation, activation, and relaxation periods are determined by considering the variability of the wind at the meridional transect that corresponds to the axis of greatest variability of the jet,

including the $PLLJ_{max}$ point. A comparative Multi-Taper (MTM) winds spectral analysis in and around the $PLLJ_{max}$ is performed as a sensitivity test to confirm the $PLLJ_{max}$ representativeness of the variability of the winds in the PLLJ region. The MTM spectra are calculated considering a bandwidth of two and three orthogonal tapers.

The spatio-temporal variability of the PLLJ is analyzed on the meridional transect that corresponds to the axis of greatest variability of the jet, including the $PLLJ_{max}$ point, using the MTM. This method uses a set of independent spectral estimates based on orthogonal filters that improve the determination of the frequency spectrum of a signal and reduce a spectral loss (Ribera & Mann 2003). The MTM method has been widely applied to geophysical signal analysis problems, including analyzing instrumental data on the atmosphere and oceans (Ghil et al. 2002).

The wind time series in the $PLLJ_{max}$ is standardized and low-pass filtered using a Cosine-Lanczos filter with a cut-off period of 1.5 years to observe low-frequency variations associated with ENSO phenomena in the 3-7 years band. The filtered series is correlated with the Niño 1+2 ocean index, which is the spatial average of sea surface temperature anomalies in an area between 0-10°S and 90-80°W (Rayner 2003). This index was chosen because it correlates with ENSO coastal events in southern Colombia (Rodríguez-Rubio 2013). Similar filtering and correlation processes were performed with the PLLJ extension series.

A wavelet spectrum is performed in the meridional and zonal wind components to analyze the persistence of the wind speed perturbations in the PLLJ at different time scales, using a Morlet window, following the algorithms of Torrence & Compo (1998) and Grinsted et al. (2004). The resulting wavelet spectrum shows on the *x*-axis the time associated with the wind series, on the *y* axis the frequencies (or periods) of variability, and the color scale represents the energy associated with each frequency or period.

RESULTS

Extension and annual cycle of the PLLJ

In the ETPC, the PLLJ generates a high energy area due to the high variability of the winds, as is observed in the standard deviation field calculated on 26 years of satellite wind data (Fig. 2a). Considering the isoline of standard deviation (SD) ± 2.10 m s^{-1}, the PLLJ high-variability zone extends between 81°0'0"-78°48'0"W and 5°0'0"-8°0'0"N. Within this zone, the point of greatest intensity ($PLLJ_{max}$) presented a standard deviation greater than 2.37 m s^{-1} and was located at 79°11'15"W and 7°48'45"N (black triangle, Figs. 2a-b).
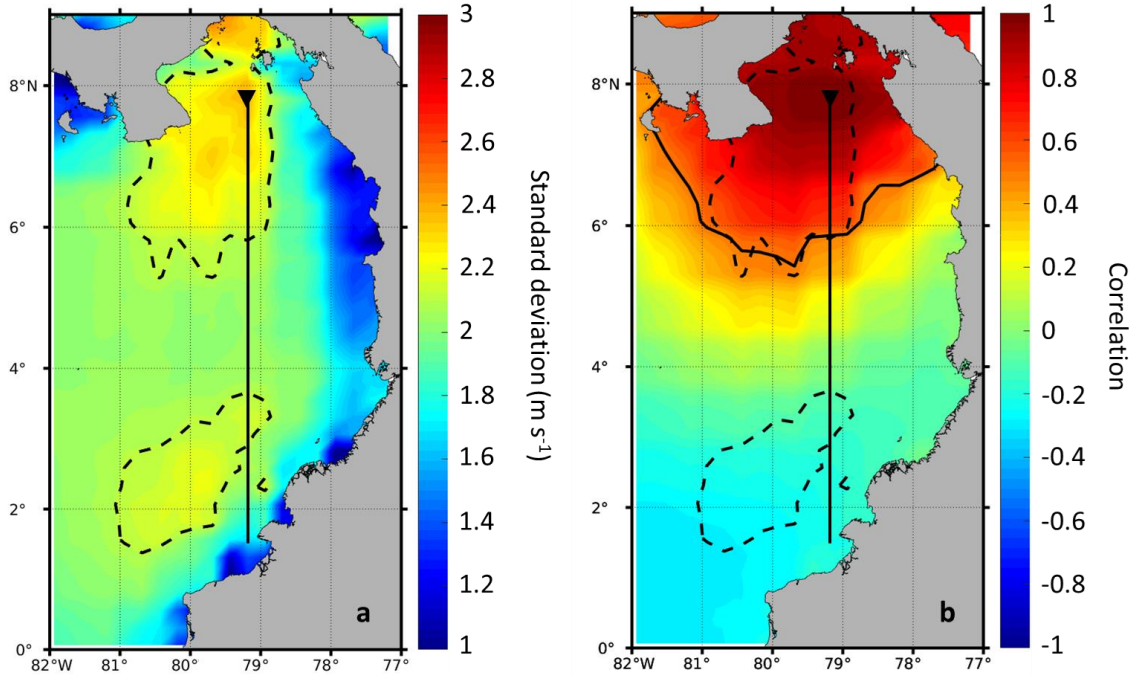
Figure 2. a) ETPC wind variability field calculated from the 26-year standard deviation of wind speed data IFREMER-CERSAT 1992-2018. The triangle indicates the highest variability of the winds in the area of influence of the Panama Low-Level Jet (PLLJ$_{max}$), b) wind correlation field concerning the PLLJ$_{max}$. The black dashed line indicates the isoline of 2.10 standard deviations representing the PLLJ high-variability zone which extends between 81°0'0"-78°48'0"W and 5°0'0"-8°0'0"N. The solid black line indicates the isoline of 0.5 correlation. The solid grey line represents the latitudinal transect.

The spectral analysis of the wind speed shows higher energy associated with the variability of the wind in the PLLJ$_{max}$ compared to the winds in the rest of the PLLJ region, especially associated with the interannual band (2-3 years) and at seasonal, intraseasonal (around four months) and synoptic scales. Therefore, the winds in the PLLJ$_{max}$ allow a more precise estimate of the annual cycle of the PLLJ and a better description of the PLLJ variability (Fig. 3). Outside the PLLJ, the second zone of high wind variability is observed between 2-3°N, possibly linked to the variability of SWTW. The latitudinal transect on the PLLJ major variability axis was conveniently extended to this second variability zone to compare the PLLJ variability with that observed in SWTW in subsequent analyses (dotted black line, Fig. 1).

The correlation field of the winds in the ETPC concerning the PLLJ$_{max}$ presented correlations greater than 0.5 ($P < 0.01$) in an area of a similar location but with greater zonal extension (81°48'0"-77°30'0"W) than the PLLJ high-variability zone. The extent of the PLLJ high-correlation zone represents the region where the temporal variability of the winds is synchronized and consistent with the PLLJ temporal variability. Outside this region, the correlation was less than 0.2
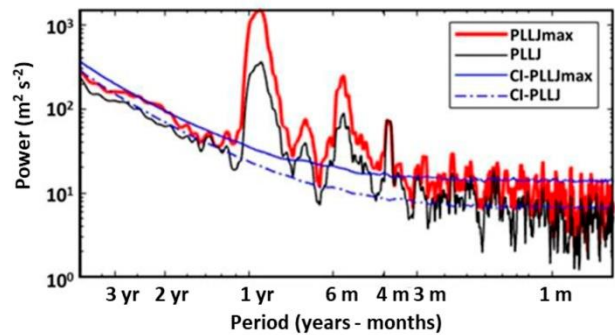
Figure 3. Comparison of the Multi-Taper spectra for the wind speeds in the PLLJ$_{max}$ (red line) and the average wind speeds within the PLLJ region (black line), calculated from 1000 iterations of the original time series. Solid and dashed blue lines correspond to the 95% confidence intervals (CI) for the PLLJ$_{max}$ spectrum and the PLLJ region spectrum, respectively.

and inverse south of 4°N, showing that winds in the SWTW region has an opposite phase concerning the PLLJ winds (Fig. 2b). Considering both the high-variability and high-correlation areas associated with the PLLJ, it is possible to observe that the effective influence area of the PLLJ is restricted between
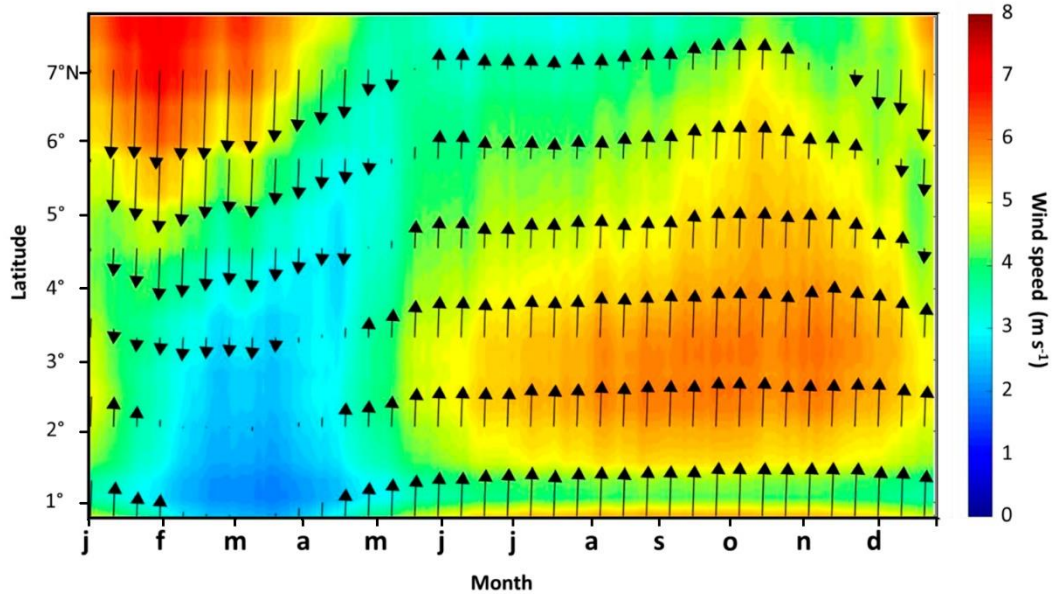
Figure 4. Annual cycle of the Panama Low-Level Jet (PLLJ) winds speeds calculated at PLLJ$_{max}$. The arrows indicate the wind magnitude and direction at 10 m from the surface. IFREMER-CERSAT data 1992-2018.

4°37'48"-9°0'0"N and has an extension of approximately 59,295.34 km².

The annual cycle of speeds calculated on the transect shows that the PLLJ is not an active wind system throughout the year. The PLLJ only activates between December and April (Fig. 4), when the low-pressure belt of the ITCZ reaches its southernmost seasonal position (Waliser & Gautier 1993, Rodríguez-Rubio et al. 2003, Devis-Morales et al. 2008). During this period, winds at the PLLJ reach their maximum speed of 8 m s^{-1} in January, extending towards south beyond 4°N, and then gradually weaken until reaching their seasonal minimum in May when the intensification of the SWTW begins.

Variation modes of the PLLJ

The variability of the winds inside and outside the PLLJ influence area was analyzed using a convoluted MTM spectrum on a north-south transect centered on the PLLJ$_{max}$ (79°22'30"W, red line, Fig. 1). This spectrum shows a minimum of spectral power at 4°7'30"N (dashed line, Fig. 5). Towards the north of this latitude, more frequency components are observed inside the PLLJ region, both in the inter-annual band (Fig. 5a) and the intra-seasonal band (Figs. 5c-d), concerning the southern region of 4°7'30"N corresponding to SWTW, latitude that coincides with the southern limit of the PLLJ high-variability zone (Fig. 5e). Thus, the PLLJ has intra-seasonal variability components (one to five months) that are not observed in the SWTW, which are

oscillations usually associated with Madden-Julian phenomena (Zhang 2005). Although the annual and semi-annual (six months) frequencies of variability are significant throughout the transect, they are more energetic in the SWTW than in the PLLJ (Figs. 5b-c). In the inter-annual band, frequency components between two to six years are observed with more energy in the PLLJ region and could be related to an intensified modulation of the winds by the ENSO phenomena. The greater number of variability components observed in the PLLJ could be an important source of atmospheric variability within the ETPC region, which can be transmitted, and affect the ocean heat content and circulation.

Modulation of the extent and intensity of the Panama jet by ENSO events

The Hovmoeller diagram of the wind speed during the periods of the PLLJ activation (December to April) shows an inter-annual variability in the intensity, extent, and duration of the PLLJ activity season. During years of stronger winds, the spatial range of the PLLJ extends south of 2ºN (Fig. 6a), even affecting the southern Pacific coast of Colombia. Moreover, the Hovmoeller diagram associated with periods of PLLJ relaxation (March to November) shows that the SWTW are less intense before periods associated with a high energy activation of the jet; on the other hand, SWTW increase in intensity before low energy activation (Fig. 6b).
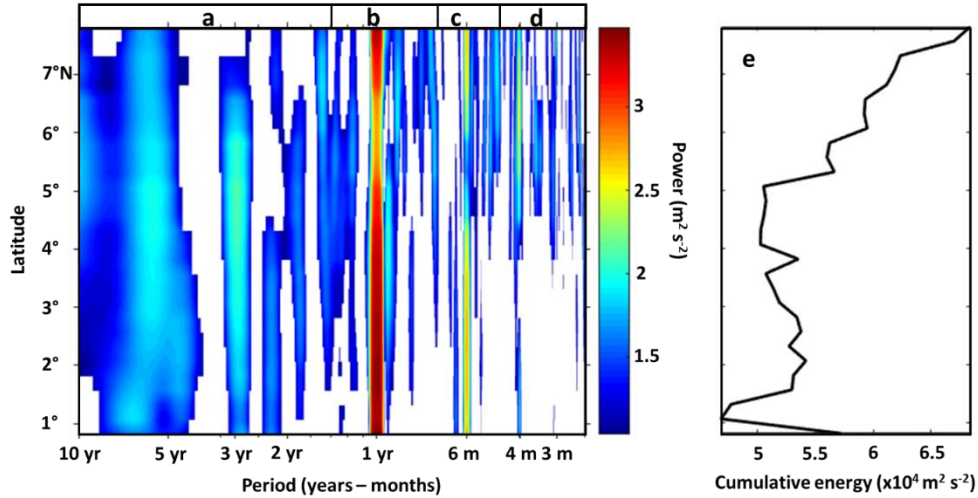
Figure 5. Multi-Taper moving spectrum of the wind speed over the Panama Low-Level Jet (PLLJ$_{max}$) latitudinal transect (79°22'30"W, 8°22'30"-1°22'30"N). Temporal bands of the spectrum: a) inter-annual, b) annual, c) semi-annual, and d) intra-seasonal. Tone colors represent the energy level for each frequency. Non-significant frequencies below 99% of the confidence level are left blank. Confidence levels are obtained by bootstrapping and performing several permutations of the original time series. e) Cumulative spectral energy by latitude (in arbitrary units), where the dashed line shows the latitude of the minimum energy observed at the southern edge of the PLLJ (4°7'30"N).
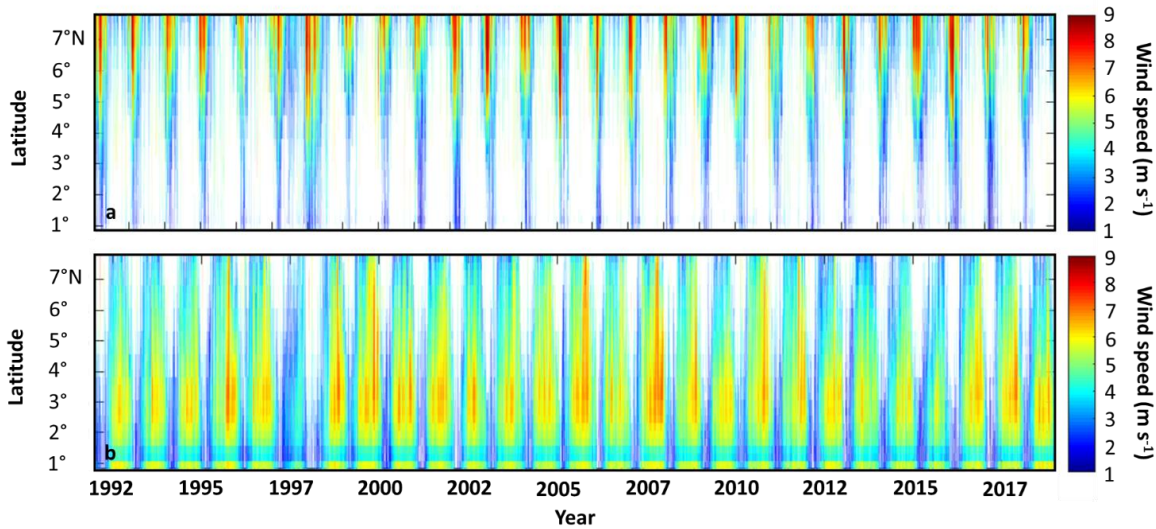
Figure 6. Wind speed in m s^{-1} in the transect (79°22'30"W, 8°22'30"-1°22'30"N). a) The periods with the presence of south winds are excluded and left blank to highlight only the winds associated with the Panama Low-Level Jet, b) the periods with the presence of north winds are excluded and left blank, to highlight only the winds associated with the Southwest Trade Winds.

The occurrence of ENSO events has a significant and positive correlation with the standardized anomaly of the PLLJ extension ($r = 0.86$, $P < 0.01$), however, with the velocity, this correlation was not as intense ($r = 0.10$, $P < 0.01$) (Fig. 7). This result shows that ENSO impacts the extension more than the intensity of the PLLJ, with no lags regarding the coastal ENSO indices. Therefore, if warm ENSO events coincide with the jet

activity season, there is an increase in the jet extension in the ETPC; on the contrary, if cold ENSO events occur, the effective jet area is reduced.

Additionally, ENSO also affects the onset and duration of the PLLJ activity season. During the ENSO warm phase, the jet season exhibits a bimodal behavior, with the first period of activity from mid-November to mid-May when it remains active for six months, and
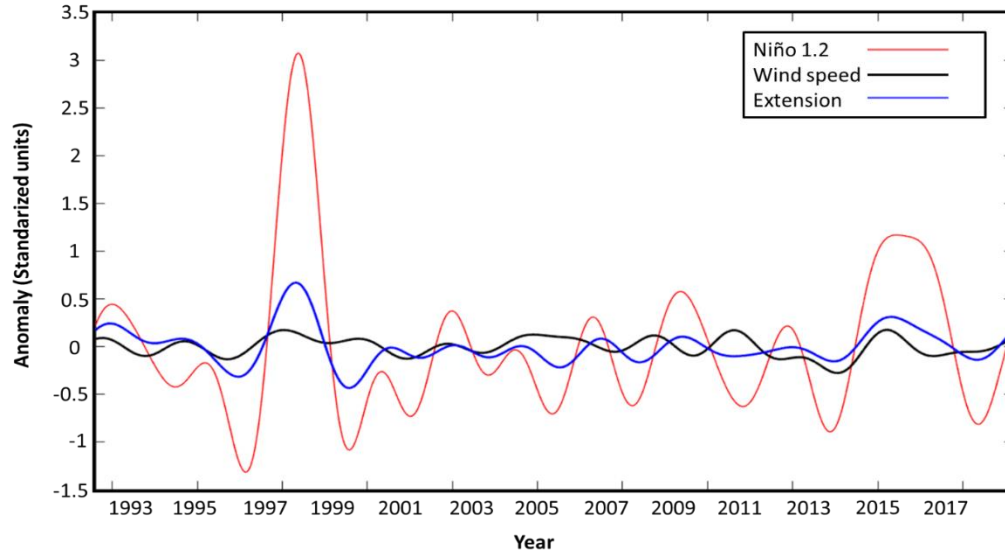
Figure 7. Standardized and filtered anomalies of extension (blue) and wind speed (black) of the Panama Low-Level Jet and Niño 1.2 index (red). The wind speed was taken at PLLJ$_{max}$ at 1013 hPa.

with a second activation during the boreal summer months, this is represented by the black line in Figure 8a that shows the 0 m s^{-1} contour of the meridional component of the wind speed, which remains negative (north to south) during the activation. In years corresponding to the cold ENSO phase, the jet duration is like its climatology, remaining active only five months in a unique period, from mid-November to April (Fig. 8b).

The previously described ENSO effects on the PLLJ can be seen in more detail (Figs. 9 a-d). Changes in the wind velocity and direction in the PLLJ$_{max}$ during warm and cold events are shown more explicitly in this figure than those observed in the smoothed annual cycles of Figure 8. During the cold ENSO years of 1999 and 2010 (Figs. 9a-b), the activity of the jet resemblances its climatology, with a unique intensification period between December through May reaching velocities of 10 m s^{-1} from the north northeast (NNE) and a relaxation interval on the rest of the year. However, the activation pattern of the PLLJ changes during the warm ENSO years of 1997 and 2015 (Figs. 9c-d); although the first activation period is similar to the climatology, a second intensification is observed during the boreal summer months, especially in July-August, but with less intense winds (5 m s^{-1}) also coming from the NNE.

Wavelet decomposition of the PLLJ

The wavelet analysis shows the influence of the inter-annual variability present on the zonal wind component at the PLLJ$_{max}$ (Fig. 10a). Using the bias of the PLLJ
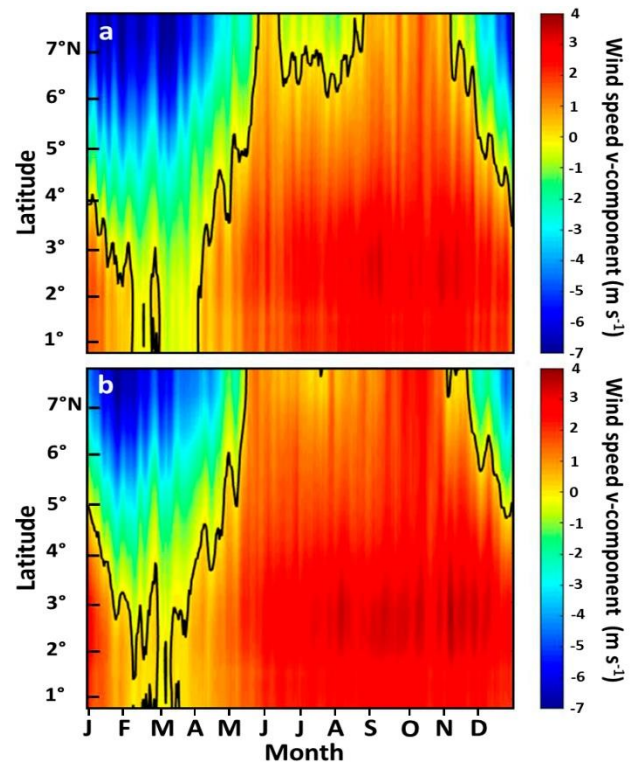
Figure 8. Annual cycle of the wind speed in m s^{-1} in the transect (79°22'30"W, 8°22'30"-1°22'30"N) at 1013 hPa, for corresponding years with ENSO events a) warm and b) cold. The solid black line represents the 0 m s^{-1} contour of the north-south component of the wind; negative values enclose the activation periods of the Panama Low-Level Jet. During warm/cold events, the isoline shows/hides extension peaks in the boreal summer months.
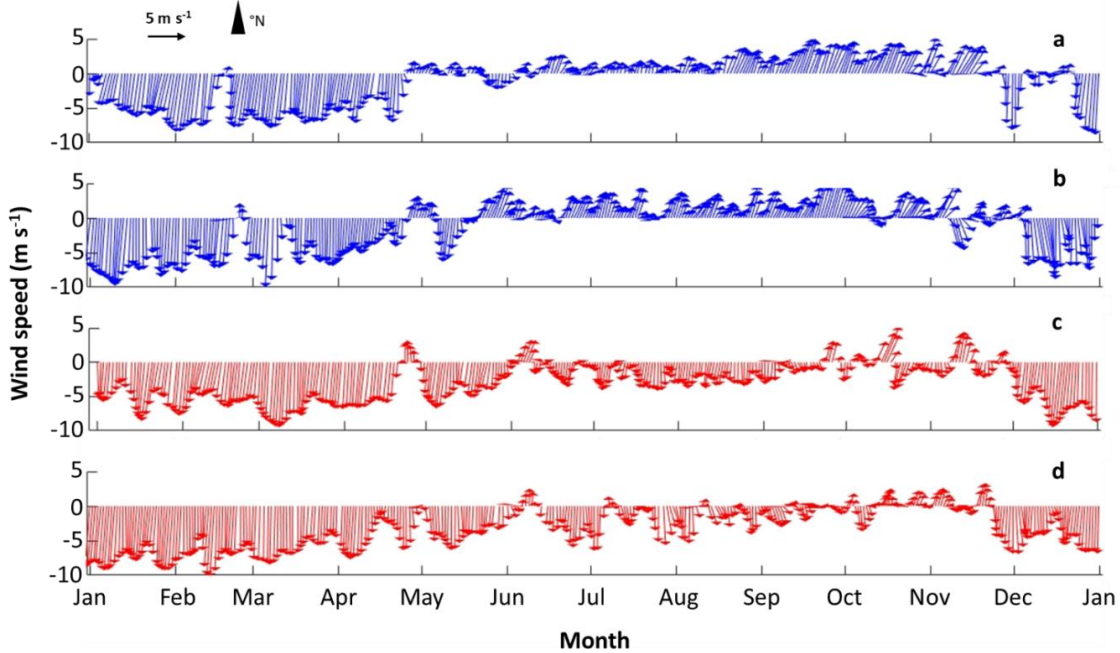
Figure 9. Wind speed and direction in Panama Low-Level Jet (PLLJ$_{max}$) during ENSO year activity. Cold events in blue, a) 1999 and b) 2010. Warm events in red, c) 1997 and d) 2015.
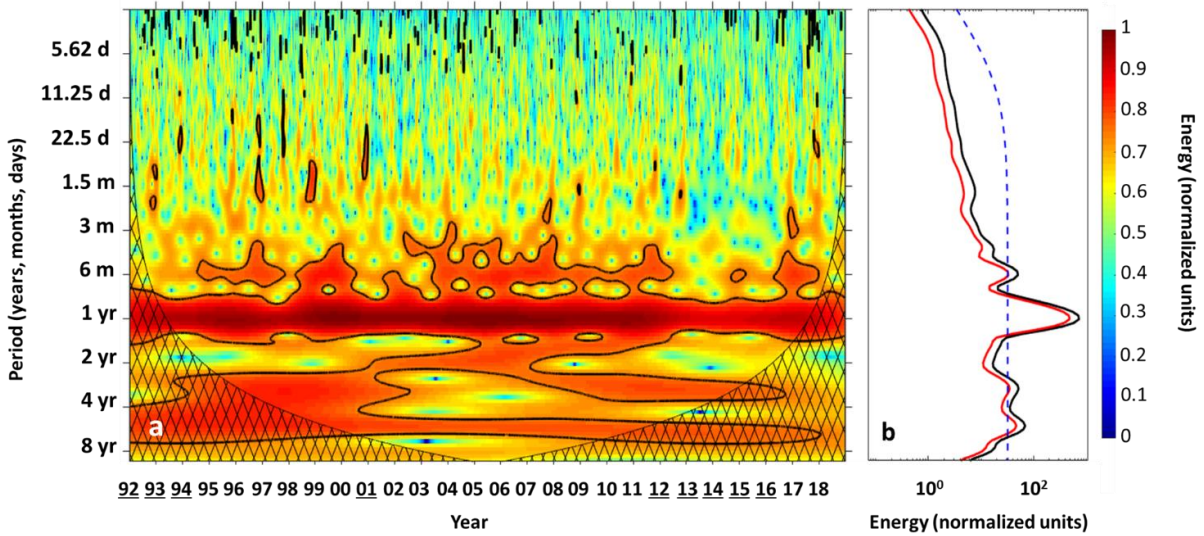
Figure 10. a) Wavelet spectra of the zonal wind speed of the Panama Low-Level Jet. Wavelet spectrum with lines above 95% significance, the underlined section represents the cone of influence area over which the analysis is no longer significant. Tone colors represent the energy level for each period. The underlined years correspond to the semi-annual signal gaps mentioned in the text. In the total wavelet spectrum b), the red line represents the energy of the meridional component during the jet activation periods; the black line corresponds to the energy of the entire sampling period, and the blue dashed line the 95% significance level. IFREMER-CERSAT data 1992-2018.

activation periods, it is observed that inter-annual frequencies significantly contribute to the jet velocities and can determine intensification patterns associated with events that have this periodicity (red curve, Fig. 10b). The wavelet analysis showed that in some years

(1992-1994, 2001, 2012-2016), the magnitude of the semi-annual cycle does not exceed the background noise level, becoming insignificant. It also occurs with the intra-seasonal variability, whose origin may be associated with the zonal transport caused by Madden-
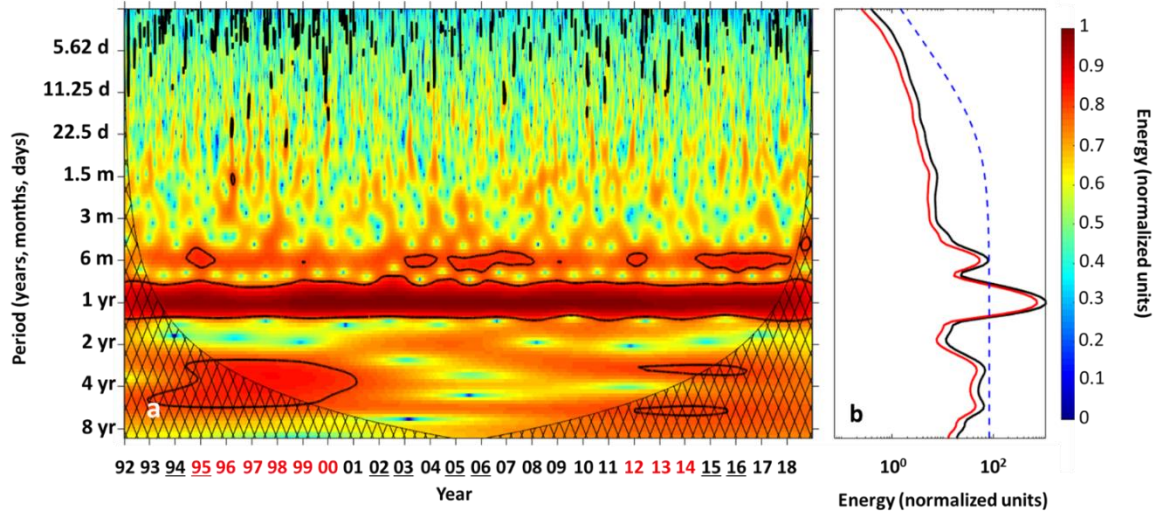
Figure 11. a) Wavelet spectra of the meridional velocity component of the Panama Low-Level Jet. Spectrum with lines above 95% significance, the underlined section represents the cone of influence, an area over which the analysis is no longer significant. Tone colors represent the energy level for each period. The underlined years correspond to the semi-annual signals mentioned in the text; the red ones are the years with intense inter-annual activity. In the total wavelet spectrum b), the red line represents the energy of the zonal component during the jet activation periods, the black line corresponds to the energy of the entire sampling period, and the blue dashed line the 95% significance level. IFREMER-CERSAT data 1992-2018.

Julian oscillation in the western Pacific (Zhang 2005), which is reduced during these years.

On the other hand, the wavelet analysis of the meridional velocity at PLLJ$_{max}$ showed that the annual band frequency is more continuous and has higher energy in the meridional wavelet than in the zonal wavelet (Fig. 11a). In contrast, the semi-annual band of the meridional wavelet was not significant in almost all years, except in the boreal summer of the El Niño years 1994, 1996/1997, 2002, 2005/2006, and 2015/2016. The meridional wavelet also showed fewer energy signals in the intra-seasonal band (30 to 90 days) and an increased number of signals in the synoptic band (1 to the 5.62-day band) than those observed in the zonal wavelet. The total wavelet spectrum of the meridional component showed less energy in the inter-annual band than zonal wavelet (Fig. 11b), with significant energy increases in the years 1995-2000 and 2010-2016, all of them characterized by an intense ENSO activity; especially El Niño 1997/1998 (Trenberth et al. 2002), La Niña 2010/2011 (Hoyos et al. 2013) and El Niño 2015/2016 (Martínez et al. 2017).

Wavelet analysis results also suggest the second activation of the PLLJ during the boreal summer when intense warm ENSO events occur. This secondary activation can be observed as sudden speed changes in the meridional wind occurring in the years 1994, 1996/1997, 2002, 2005/2006, when meridional winds

intensify towards the south generating significant signals (above 95%) in the semi-annual band of the meridional wavelet (Fig. 11a). The timing of these secondary activation coincides with the intensification of the north trade winds over the Caribbean basin in the middle of the year (Bernal et al. 2006) caused by the semi-annual variation of the SST and pressure gradients in the southern Caribbean (Wang 2007). The secondary activation of the PLLJ has a reduced area of influence, showing its highest wind speeds north of 6°N.

DISCUSSION

Analysis of the wind magnitude and direction data showed an extensive area of high variability and energy directly associated with the seasonal activation of PLLJ, whose extension represents around 0.6% of the Eastern Tropical Pacific (which, according to Redfern et al. 2008, has 19.6 million of km^2) and more than 30% of the ETPC. The PLLJ borders to the south with another area of high wind variability dominated by SWTW, which has a seasonal cycle opposite the PLLJ winds. The seasonal peak of SWTW occurs between May and September, when the ITCZ is in its northern-most position (Forsbergh 1969, Waliser & Gautier 1993, Rodríguez-Rubio et al. 2003, Timmermann et al. 2010, Amador et al. 2016) and when the PLLJ is inactive. In these months, the SWTW covers almost the

entire ETPC, also including the PLLJ area. When the ITCZ moves south, the SWTW decreases until it almost disappears, and the PLLJ is activated. Therefore, the ETPC is a region dominated by two wind regimes whose climatic variability is opposite; they have different variability components and connect the basin with the variability of the Pacific and the Caribbean. Although the main frequencies of variability in the SWTW are mostly annual and semi-annual, the PLLJ also presents additional frequencies of variability in the inter-annual and intra-seasonal bands, which could correspond to processes in the Caribbean (Schultz et al. 1998) or even atmospheric teleconnections with Pacific ENSO variability (Mora & Amador 2000).

The PLLJ is bordered to the east by Chocó Low-Level Wind Jet (Poveda & Mesa 1999), a coastal wind jet that peaks annually in September-October-November at the end of the SWTW season, and therefore its annual cycle is also inverse to that of the PLLJ. The Chocó Jet flows north parallel to the west coast of South America and turns east when it crosses the equator, transporting a large amount of moisture $(11.9 \times 10^{13}$ kg yr^{-1}) to the rainfall into Colombia (Poveda & Mesa 1999, Arias et al. 2015, Hoyos et al. 2018, Serna et al. 2018). Like that observed in the PLLJ, the intensity of the Chocó Jet appears to be controlled by the gradient of sea surface temperatures between the El Niño1+2 regions (Poveda 1998). The relationship between Choco Jet and PLLJ has not yet been analysed, but it could contribute to understanding the connection of the Pacific with the continental climate in Colombia.

In addition to seasonal and inter-annual variability, the winds in the PLLJ present many frequencies of variability in the intra-seasonal band (30-120 days) that are not as significant in the SWTW. These frequencies are usually associated with Madden-Julian waves, atmospheric structures traveling eastward at tropical latitudes that affect the Colombian Pacific and Caribbean basin climate (Rivera-Páez & Molares-Babra 2003, Poveda 2004, Zhang 2005). Previous studies have attempted to quantify a relationship between the Madden-Julian index and climatic indices in the Colombian Pacific. Although common frequencies have been found in the intra-seasonal bands (30-60 days), a low Madden-Julian influence has been observed, at least in the case of the precipitation on the Colombian territory (Torres-Pineda & Pabón-Caicedo 2017). However, strong atmospheric intra-seasonal variability has been observed in the intensification of tropical cyclones in the Pacific associated with the intensification of the southern component of the wind during the passage of a Madden-Julian cell (Klotzbach & Blake 2013). Future climatic analyses considering the two wind regimes of the ETPC could allow better discrimination of Madden-Julian influence in the atmospheric circulation and climate of the region.

This study showed that inter-annual disturbances of winds associated with ENSO in the ETPC occur mostly in the influence area of the PLLJ. This jet presents significant and highly energetic components in the inter-annual frequency within the quasi-quadrennial variance band centered in a 3-6 years period and a weaker and intermittent one in a quasi-biennial band with a variance centered in 2-3 years, typical frequencies associated to ENSO variability (Ribera & Mann 2003). The effect of ENSO in the Pacific has been extensively documented. Especially on the increase of the tropical cyclones during the warm phase, which conversely reduces their intensity and occurrence during the cold phase (Klotzbach & Blake 2013, Fu et al. 2017), due to the anomalous disturbances of the trade winds in the equatorial Pacific that modify the zonal distribution of the ocean heat between the warm and cold phases of the ENSO (Fedorov & Brown 2009, Brown & Fedorov 2010). Our results show an increase in the PLLJ extension during ENSO warm events. This increase could be linked to the weakening of the Eastern Trade Winds and the intensification of the low-pressure center due to the positive temperature anomalies on the ETPC (Rasmusson & Carpenter 2002, Sheinbaum 2003, Ashok et al. 2007).

The present study reports for the first time the presence of a sporadic semi-annual signal associated with extemporaneous activation of PLLJ during warm ENSO events. This pattern contrasts with previous studies reporting a unimodal annual pattern of intensification and relaxation (Rueda-Bayona et al. 2007, Mora 2017, DIMAR 2020). Furthermore, our results reinforce the hypothesis that some variations of the intra-American jets are correlated with the trade winds over the Caribbean (Chelton et al. 2000b). Therefore, intensification of the CLLJ in the boreal summer could be linked to the eventual onset of PLLJ in this scale period. This connection has also been observed in high-frequency synoptic events from the Caribbean that produce biological and oceanographic effects on ETPC, and these events are linked to cold fronts with a persistence between two and six days (Schultz et al. 1998, Liang et al. 2009).

The new estimates reported in this study on the extent of the PLLJ may be important to operational and logistic purposes in the ETP. The PLLJ extent not only determines the region's climatic patterns but can also be useful to the naval trade or to identify potential regions that can be considered for resource-use research, for example, for the generation of eolic energy with

offshore wind turbines. The new patterns reported in this study regarding the influence of ENSO on PLLJ must be considered at the time of future engineering designs or maritime operations in the ETPC.

ACKNOWLEDGMENTS

REFERENCES

Alexander, M.A., Seo, H., Xie, S.P. & Scott, J.D. 2012. ENSO's impact on the gap wind regions of the eastern tropical Pacific Ocean. Journal of Climate, 25: 3549-3565.

Amador, J.A. 1998. A climatic feature of the tropical Americas: the trade wind easterly jet. Tópicos Meteorológicos y Oceanográficos, 5: 1-13.

Amador, J.A., Durán-Quesada, A.M., Rivera, E.R., Mora, G., Sáenz, F., Calderón, B. & Mora, N. 2016. The easternmost tropical Pacific. Part II: Seasonal and intraseasonal modes of atmospheric variability. Revista de Biología Tropical, 64: 23-57.

Arias, P.A., Martínez, J.A. & Vieira, S.C. 2015. Moisture sources to the 2010-2012 anomalous wet season in northern South America. Climate Dynamics, 45: 2861-2884.

Ashok, K., Behera, S.K., Rao, S.A., Weng, H. & Yamagata T. 2007. El Niño Modoki and its possible teleconnection. Journal of Geophysical Research: Oceans, 112: C11007. doi: 10.1029/2006JC00 3798, 2007

Bernal, G., Poveda, G., Roldán, P. & Andrade, C. 2006. Patrones de variabilidad de las temperaturas superficiales del mar en la costa Caribe colombiana. Revista de la Academia Colombiana de Ciencias Exactas, Físicas y Naturales, 30: 195-208.

Brown, J.N. & Fedorov, A.V. 2010. How much energy is transferred from the winds to the thermocline on ENSO time scales? Journal of Climate, 23:1563-1580.

Chelton, D.B., Freilich, M.H. & Esbensen, S.K. 2000a. Satellite observations of the wind jets off the Pacific coast of Central America. Part I: Case studies and statistical characteristics. Monthly Weather Review, 128: 1993-2018.

Chelton, D.B., Freilich, M.H. & Esbensen, S.K. 2000b. Satellite observations of the wind jets off the Pacific coast of Central America. Part II: Regional relationships and dynamical considerations. Monthly Weather Review, 128: 2019-2043.

Devis-Morales, A., Schneider, W., Montoya-Sánchez, R.A. & Rodríguez-Rubio, E. 2008. Monsoon-like winds reverse oceanic circulation in the Panama Bight. Geophysical Research Letters, 35. doi: 10.1029/2008 GL035172

Dirección General Marítima (DIMAR). 2020. Compilación oceanográfica de la Cuenca Pacífica Colombiana II. Serie publicaciones especiales CCCP, Vol. 9. Editorial DIMAR, Bogotá.

Fedorov, A.V. & Brown, J.N. 2009. Equatorial waves. In: Steele, J. (Ed.). Encyclopedia of ocean sciences. Academic Press, New York, pp. 3679-3695.

Forsbergh, E.D. 1969. On the climatology, oceanography and fisheries of the Panama Bight Inter-American Tropical Tuna Commission Bulletin, 14: 46-385.

Francis, D., Fonseca, R., Nelli, N., Cuesta, J., Weston, M., Evan, A. & Temimi, M. 2020. The atmospheric drivers of the major Saharan dust storm in June 2020. Geophysical Research Letters, 47: e2020GL090102.

Fu, D., Chang, P. & Patricola, C.M. 2017. Intrabasin variability of east Pacific tropical cyclones during ENSO regulated by Central American gap winds. Scientific Reports, 7: 1-8.

Ghil, M., Allen, M.R., Dettinger, M.D., Ide, K., Kondrashov, D., Mann, M.E., et al. 2002. Advanced spectral methods for climatic time series. Reviews of Geophysics, 40: 1-3.

Grinsted, A., Moore, J.C. & Jevrejeva, S. 2004. Application of the cross wavelet transform and wavelet coherence to geophysical time series. Nonlinear Processes in Geophysics, 11: 561-566.

Hoyos, N., Escobar, J., Restrepo, J.C., Arango, A.M. & Ortiz, J.C. 2013. Impact of the 2010-2011 La Niña phenomenon in Colombia, South America: the human toll of an extreme weather event. Applied Geography, 39: 16-25.

Hoyos, I., Domínguez, F., Cañón-Barriga, J., Martínez, J.A., Nieto, R., Gimeno, L. & Dirmeyer, P.A. 2018. Moisture origin and transport processes in Colombia, northern South America. Climate Dynamics, 50: 971-990.

Jakobson, L., Vihma, T., Jakobson, E., Palo, T., Männik, A. & Jaagus, J. 2013. Low-level jet characteristics over the Arctic Ocean in spring and summer. Atmospheric Chemistry and Physics, 13: 11089-11099.

Klotzbach, P.J. & Blake, E.S. 2013. North-Central Pacific Tropical cyclones: impacts of El Niño-Southern Oscillation and the Madden-Julian Oscillation. Journal of Climate, 26: 7720-7733. doi: 10.1175/JCLI-D-12-00809.1

Laing, A. & Evans, J. L. 2010. Introduction to tropical meteorology: a comprehensive online and print textbook. Version 2a. COMET Program, University Corporation for Atmospheric Research. [http//:www.meted.ucar.edu/tropical/textbook_2nd_edition]. Reviewed: March 15, 2020.

Langland, R.H., Tag, P.M. & Fett, R.W. 1989. An ice breeze mechanism for boundary-layer jets. Boundary-Layer Meteorology, 48: 177-195.

Liang, J., McWilliams, J.C. & Gruber, N. 2009. High-frequency response of the ocean to mountain gap winds in the northeastern tropical Pacific. Journal of Geophysical Research: Oceans, 114: C12005. doi: 10.1029/2009JC005370,2009

Martínez, R., Zambrano, E., Nieto, J.J., Hernández, J. & Costa, F. 2017. Evolución, vulnerabilidad e impactos económicos y sociales de El Niño 2015-2016 en América Latina. Investigaciones Geográficas, 68: 65-78.

Mora, G. 2017. Climatology of the low-level winds over the intra-americas sea using satellite and reanalysis data. Tópicos Meteorológicos y Oceanográficos, 16: 15-30.

Mora, I. & Amador-Astúa, J.A. 2000. El ENOS, el IOS y la corriente en chorro de bajo nivel en el oeste del Caribe. Tópicos Meteorológicos y Oceanográficos, 7: 1-20.

Muñoz, E., Busalacchi, A.J., Nigam, S. & Ruiz-Barradas, A. 2008. Winter and summer structure of the Caribbean Low-Level Jet. Journal of Climate, 21: 1260-1276.

O'Dea, A., Hoyos, N., Rodríguez, F., Degracia, B. & De Gracia, C. 2012. History of upwelling in the Tropical Eastern Pacific and the paleogeography of the Isthmus of Panama. Paleogeography, Palaeoclimatology, Palaeoecology, 348: 59-66.

Pezzi, L.P. & Cavalcanti, I.F.A. 2001. The relative importance of ENSO and tropical Atlantic sea surface temperature anomalies for seasonal precipitation over South America: a numerical study. Climate Dynamics, 17: 205-212.

Poveda, G. 1998. Retroalimentación dinámica entre el Fenómeno El Niño-Oscilación del Sur y la hidrología de Colombia. Universidad Nacional de Colombia, Medellín.

Poveda, G. 2004. La hidroclimatología de Colombia: una síntesis desde la escala inter-decadal hasta la escala diurna. Revista de la Academia Colombiana de Ciencias Exactas, Físicas y Naturales, 28: 201-222.

Poveda, G. & Mesa, O. 1999. La corriente de Chorro Superficial del Oeste ("Del Chocó") y otras dos corrientes de chorro en Colombia: climatología y variabilidad durante las fases del ENSO. Revista de la Academia Colombiana de Ciencias Exactas, Físicas y Naturales, 23: 517-528.

Rai, P. & Dimri, A.P. 2017. Effect of changing tropical easterly jet, low-level jet and quasi-biennial oscillation phases on Indian summer monsoon. Atmospheric Science Letters, 18: 52-59.

Rasmusson, E.M. & Carpenter, T.H. 2002. Variations in tropical sea surface temperature and surface wind fields associated with the Southern Oscillation/El Niño. Monthly Weather Review, 110: 354-384. doi: 10.1175/1520-0493(1982)110<0354:vitsst>2.0.co;2

Rayner, N.A. 2003. Global analyses of sea surface temperature, sea ice, and night marine air temperature since the late nineteenth century. Journal of Geophysical Research, 108. doi: 10.1029/2002jd002670

Redfern, J.V., Barlow, J., Balance, L.T., Gerrodette, T. & Becker, E.A. 2008. Absence of scale dependence in dolphin-habitat models for the eastern tropical Pacific Ocean. Marine Ecology Progress Series, 363: 1-14.

Renfrew, I.A. & Anderson, P.S. 2006. Profiles of katabatic flow in summer and winter over Coast Land, Antarctica. Quarterly Journal of the Royal Meteorological Society, 132: 779-802.

Ribera, P. & Mann, M.E. 2003. ENSO related variability in the Southern Hemisphere, 1948-2000. Geophysical Research Letters, 30: 1-6.

Rivera-Páez, S. & Molares-Babra, R.J. 2003. Evidencias de la oscilación del tiempo Madden-Julian en el Caribe colombiano. Boletín Científico CIOH, 21: 101-113.

Rodríguez-Rubio, E. 2013. A multivariate climate index for the western coast of Colombia. Advances in Geosciences, 33: 21-26.

Rodríguez-Rubio, E., Schneider, W. & Abarca del Río, R. 2003. On the seasonal circulation within the Panama Bight derived from satellite observations of wind, altimetry and sea surface temperature. Geophysical Research Letters, 30: 1410. doi:10.1029/2002GL016794, 2003

Romero-Centeno, R., Zavala-Hidalgo, J., Gallegos, A. & O'Brien, J.J. 2003. Isthmus of Tehuantepec wind climatology and ENSO signal. Journal of Climate, 16: 2628-2639.

Ropelewski, C.F. & Halpert, M.S. 2002. Global and regional scale precipitation patterns associated with

the El Niño/Southern Oscillation. Monthly Weather Review, 115: 1606-1626. doi: 10.1175/1520-0493 (1987)115<1606:garspp>2.0.co;2

Rueda-Bayona, J.G., Rodríguez-Rubio, E. & Ortiz-Galvis, J.R. 2007. Caracterización espacio temporal del campo de vientos superficiales del Pacífico colombiano y el Golfo de Panamá a partir de sensores remotos y datos in situ. Boletín Científico CCCP, 14: 49-68.

Sáenz, F. & Durán-Quesada, A.M. 2015. A climatology of low-level wind regimes over Central America using a weather type classification approach. Frontiers in Earth Science, 3: 15. doi: 10.3389/feart.2015.00015

Schultz, D.M., Bracken, W.E. & Bosart, L.F. 1998. Planetary-and synoptic-scale signatures associated with Central American cold surges. Monthly Weather Review, 126: 5-27.

Serna, L.M., Arias, P.A. & Vieira, S.C. 2018. Las corrientes superficiales de chorro del Chocó y el Caribe durante los eventos de El Niño y El Niño Modoki. Revista de la Academia Colombiana de Ciencias Exactas, Físicas y Naturales, 42: 410-421.

Sheinbaum, J. 2003. Current theories on El Nino-southern oscillation: a review. Geofísica Internacional, 42: 291-305.

Small, R.J.O., De Szoeke, S.P. & Xie, S-P. 2007. The Central American midsummer drought: regional aspects and large-scale forcing. Journal of Climate, 20: 4853-4873.

Smith, D., Li, X., Keiser, K. & Flynn, S. 2014. Regional Air-Sea Interactions (RASI) climatology for Central America coastal gap wind and upwelling events. Oceans-St. John's, Institute of Electrical and Electronics Engineers, New Jersey.

Stensrud, D.J. 1996. Importance of low-level jets to climate: a review. Journal of Climate, 9: 1698-1711.

Timmermann, A., McGregor, S. & Jin, F-F. 2010. Wind effects on past and future regional sea level trends in the southern Indo-Pacific. Journal of Climate, 23: 4429-4437.

Torrence, C. & Compo, G.P. 1998. A practical guide to wavelet analysis. Bulletin of the American Meteorological Society, 79: 61-78.

Torres-Pineda, C.E. & Pabón-Caicedo, J.D. 2017. Variabilidad intraestacional de la precipitación en Colombia y su relación con la oscilación de Madden-Julian. Revista de la Academia Colombiana de Ciencias Exactas, Físicas y Naturales, 41: 79-93.

Trenberth, K.E., Caron, J.M., Stepaniak, D.P. & Worley, S. 2002. Evolution of El Niño-Southern Oscillation and global atmospheric surface temperatures. Journal of Geophysical Research: Atmospheres, 107: 1-17.

Tuononen, M., Sinclair, V.A. & Vihma, T. 2015. A climatology of low-level jets in the mid-latitudes and polar regions of the Northern Hemisphere. Atmospheric Science Letters, 16: 492-499.

Turner, A.G., Inness, P.M. & Slingo, J.M. 2005. The role of the basic state in the ENSO-monsoon relationship and implications for predictability. Quarterly Journal of the Royal Meteorological Society, 131: 781-804.

Waliser, D.E. & Gautier, C. 1993. A satellite-derived climatology of the ITCZ. Journal of Climate, 6: 2162-2174.

Wang, C. 2007. Variability of the Caribbean Low-Level Jet and its relations to climate. Climate Dynamics, 29: 411-422. doi: 10.1007/s00382-007-0243-z

Xie, S-P., Xu, H., Kessler, W.S. & Nonaka, M. 2005. Air-sea interaction over the eastern Pacific warm pool: gap winds, thermocline dome, and atmospheric convection. Journal of Climate, 18: 5-20.

Yang, J-C., Lin, X. & Xie, S-P. 2017. A transbasin mode of inter-annual variability of the Central American gap winds: seasonality and large-scale forcing. Journal of Climate, 30: 8223-8235.

Zhang, C. 2005. Madden-Julian oscillation. Reviews of Geophysics, 43: 1-36. doi: 10.1029/2004R G000158